

# Development of a Diaphragm for a Planar Acoustic Transducer

by Takeshi Nishimura<sup>\*</sup>, Kenji Iizuka<sup>\*2</sup>, Hideharu Yonehara<sup>\*</sup>  
Katsutoshi Sakai<sup>\*3</sup> and Motohiro Yamane<sup>\*3</sup>

**ABSTRACT** A diaphragm has been developed to meet the need for ultra-thin acoustic transducers (less than 1 cm thick) for use in liquid-crystal TV sets and in slimline light-weight equipment for automobiles. The diaphragms, which have a voice coil formed over the whole of both surfaces of the base resin film, achieve a high level of sound quality by means of circuit design techniques using magnetostatic analysis. From the physical properties and configuration of the materials (base resin, copper coil and edges) making up the diaphragm, bass reproduction characteristics of better than 65 dB at 100 Hz were achieved through the development of band design techniques using eigen-value simulation to predict the reproduction band in the bass range. In planar acoustic transducers incorporating these diaphragms, driving force is generated over the whole surface of the flat diaphragm, which acts as a planar wave radiator, providing flat phase characteristics and sharp directionality. Other outstanding advantages are that, unlike conventional cone speakers, these acoustic transducers use no paper, resulting in superior resistance to heat and moisture and making underwater operation feasible, and that the individual sound cells are smaller, reducing howling.

## 1. INTRODUCTION

With the growth in multimedia services information is processed at high speed leading to dramatic increases in the volumes of data transmitted, but at the point at which the information is imparted to a human it must be converted either into images or into sound. And with greater demand for mobile information terminals there is a relentless pressure for equipment that is smaller, slimmer and lighter in weight. As for imaging devices, more and more use is being made of liquid-crystal and plasma display panels to achieve a slimmer profile, whereas acoustic conversion devices still rely primarily on conventional cone speakers, and have not effectively come to grips with the growing need in automotive and home electronics for equipment that is slimmer and lighter in weight.

This paper reports on the development of a diaphragm optimized for a planar acoustic transducer (so-called speaker) measuring less than 1 cm in thickness designed for mounting in liquid-crystal TV sets and other ultra-slimline information terminals, and on its success in practical applications.

## 2. DEVELOPMENTAL CONCEPT

The acoustic transducer in which the diaphragm developed in this work was intended for use is an ultrathin planar acoustic transducer, classified as a conductive type with multipoint drive, and known as a Gamuzon speaker<sup>1)</sup>. Unlike conventional cone speakers, this acoustic transducer is less than 1 cm in thickness, is lighter in weight, and is of extremely simple structure with a reduced parts count. Because of its innovative structure, however, it presented problems with respect to diaphragm materials and reliability that made it difficult to apply conventional design techniques, thus requiring the development of techniques intended specifically for the evaluation of planar acoustic transducers. In addition, restrictions imposed by the slim profile required that maximum advantage be taken of the properties of the resin material and copper used in the diaphragm, and that the 2-dimensional copper circuit structure be optimized virtually to the limit value.

### 2.1 Structure and Operating Principle of Planar Acoustic Transducer

Figure 1 shows the structure and operating principle of a planar acoustic transducer<sup>2)</sup>. A planar acoustic transducer consists of a flat yoke which doubles as the outer frame, and on which are disposed permanent magnets of alternate N and S polarity. The diaphragm and voice coil, formed integrally on a flexible printed circuit (FPC) is supported flexibly by the edges at a fixed distance from the pole faces of the magnets<sup>3)</sup>.

---

<sup>\*</sup> Components & Mounting Technology Development Dept., Ecology & Energy Lab.

<sup>\*2</sup> Organic Analysis Sec., Ecology & Energy Lab.

<sup>\*3</sup> Engineering Sec., Electronic Components Dept., Electronic Components Div.

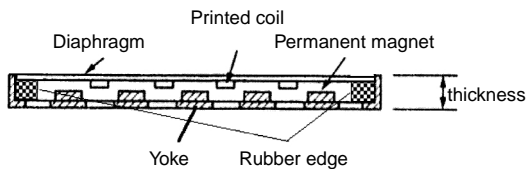


**Figure 1 Structure and operating principle of a planar acoustic transducer.**

The operating principle is as follows (see Equation (1)): In a voice coil of length  $l$  passed through a magnetic field of density  $B$ , an electrical signal (acoustic current  $I$ ) flows, and, in accordance with the principles of electromagnetic action, a driving force  $F$  is generated in a direction determined by Fleming's left-hand rule.

$$F = I l B \quad (1)$$

The voice coil is formed over the whole surface of the diaphragm, which begins a reciprocating action proportional to the changes in current flowing in the circuit, causing the air to vibrate and generating acoustic pressure.

Following are the specifications of the planar acoustic transducer in which the diaphragm under development is to be mounted, and of the diaphragm itself.

Transducer type:	FFS-0212 (2 x 12-cell array)
Outline dimensions:	40 x 160 x 8 (thick) mm
Lowest resonating frequency:	160 Hz $\pm$ 20%
Effective frequency band:	$f_0$ - 20 kHz $\pm$ 20%
Output acoustic pressure level:	82 $\pm$ 3 dB/W/m
Rated input:	7.5 W,
Input withstand:	15 W (A)
Mass:	87 g

**Diaphragm under development**

Nominal impedance:	6 $\Omega$ $\pm$ 10% or better
Continuous load tests:	JIS 96 hr, 15-25°C (8 W white noise)
Humidity tests:	40°C 90-95% RH for 96 hr
Operating ambient temperature (I)	50°C for 96 hr (8 W white noise)
Operating ambient temperature (II)	-10°C for 96 hr (8 W white noise)
Appearance of FPC	Slackness within coil not more than 0.1 mm
Additional items conform to	JPCA DG02-1997/IPC-6202.

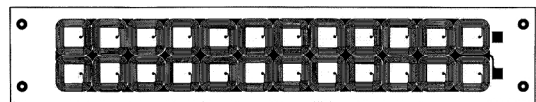


**Figure 2 Representation of a diaphragm voice coil.**

**2.2 Materials Design**

The diaphragm targeted for development, represented in Figure 2, is a flexible printed circuit board with 24 spiral coils formed on both surfaces of the base resin film in a 2 x 12-cell array, and is bonded to the acoustic transducer unit by means of flexible edges.

Among the characteristics required of the acoustic transducer diaphragm may be mentioned:

- 1) A broad reproduction frequency band and flat acoustic characteristics;
- 2) Flat phase characteristics and low distortion;
- 3) No abnormal noise or eigen-tones;
- 4) Superior environmental resistance, including heat and cold; and
- 5) No variation over time, superior durability, and freedom from open circuit faults.

Judging from conventional wisdom, an upright, slimline planar acoustic transducer measuring 40 x 160 x 8 mm might be expected to give relatively good reproduction in the mid- and high-frequency ranges but to be limited with respect to lower frequencies. If the acoustic transducer can reproduce tones as low as 100 Hz, the whole range could be covered by a one type of acoustic transducer without needing a separate woofer just for the bass. For this reason the bass reproduction capability of planar acoustic transducers will have a major significance in designing slimmer liquid-crystal TV sets. One of the targets of this development effort, therefore, was to achieve a power of 65 dB or better at 100 Hz.

Generally speaking, low-frequency characteristics are closely related to the value of bass resonance frequency  $f_0$ , which may be obtained using Equation (2)

$$f_0 = \frac{1}{2\pi} \sqrt{\frac{s}{M}} \quad [\text{Hz}] \quad (2)$$

where:  $s$  is the stiffness of the supporting portion of the vibrational system; and  $M$  is the equivalent mass of the system.

From Equation (2) we see that to reduce  $f_0$ , designs could be modified in the direction of increasing equivalent mass  $M$  and reducing support stiffness. However increasing mass  $M$  means using a thicker material for the diaphragm and increasing the weight of the copper coil, and if in fact mass is increased, rise-time characteristics will be degraded and operating efficiency will decline. The copper coil, on the other hand is subject to limitations in terms of impedance settings and methods for fabricating the printed circuits, making it difficult to change its weight at will. In general, adjustments to  $f_0$  are effected by modifying the configuration of the support structure, or edge, and by using materials with different physical properties, primarily Young's modulus.

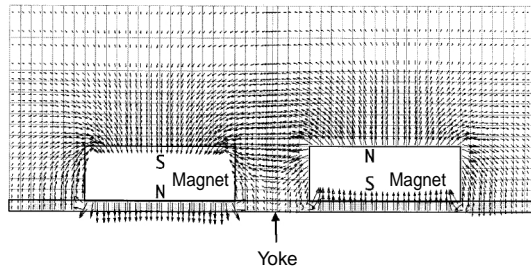


Figure 3 Results of magnetostatic analysis.

In addition, the characteristics in the bass range also depend on the sharpness  $Q_0$ , which is in turn determined primarily by the physical properties of the diaphragm material. On the other hand, since the Joule heat produced by the copper coil is transmitted directly to the base resin film of the diaphragm it is desirable that this material have good resistance to heat and humidity, as well as, from the standpoint of diaphragm characteristics, high values of specific elastic modulus ( $E/\rho$ ) and internal loss ( $\tan\delta$ ).

### 3. SIMULATED MATERIALS DESIGN AND VIBRATIONAL ANALYSIS

#### 3.1 Magnetostatic Analysis

Evaluating the acoustic performance of the diaphragm requires that an actual flat planar acoustic transducer be assembled. Thus to increase the efficiency of prototype construction and evaluation a design review was conducted by means of simulation.

In the first stage, circuit design was determined by magnetostatic analysis. The procedure adopted was to find the region of maximum magnetic flux from the arrangement of magnets on the yoke and then find a 2-dimensional space on the diaphragm such that the copper coils would be optimally disposed. Also the impedance between terminals had to be set at  $6 \Omega$ , and this dictated the length and cross-sectional area of the copper coils. Finally the optimum plating thickness and coil-to-coil distance on the edging was decided. Figure 3 is a typical result of magnetostatic analysis which was a precondition for circuit design.

As shown in Figure 1, the diaphragm developed here makes use of magnetic flux lines that parallel the pole faces of the permanent magnet, and so the coils were arranged so as to be longest in the region of highest horizontal magnetic flux density.

#### 3.2 Vibrational Mode Analysis and Eigen-value Analysis

##### 3.2.1 Analytical Method

In the second stage, in an effort to predict the diaphragm characteristics and acoustic characteristics from the properties of the materials and the configurations of components, a diaphragm analysis was carried out by means of a finite-element technique using Japan Marc Co.'s MARC

Table 1 Material characteristics and coordinate system.

	Copper coil	Film resin	Edge (hard)	Edge (soft)
Young's modulus (Pa)	$1.35 \times 10^{11}$	$4.35 \times 10^9$	$2.00 \times 10^8$	$2.00 \times 10^8$
Poisson's ratio	0.33	0.47	0.40	0.40
Density ( $\text{kg/m}^3$ )	$6.10 \times 10^3$	$1.40 \times 10^3$	$9.60 \times 10^2$	$4.80 \times 10^2$
Thickness (m)	$5.6 \times 10^{-5}$	$8.5 \times 10^{-5}$	$5.0 \times 10^{-4}$	$5.0 \times 10^{-4}$

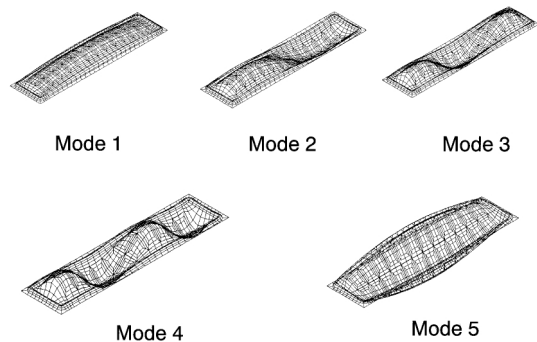
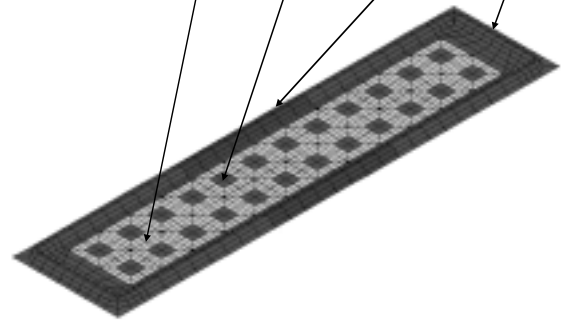


Figure 4 Vibrational mode analysis of a planar acoustic transducer diaphragm by the finite element method.

program. The fundamental equation may be stated as

$$(K - \omega^2 M)\phi = 0 \quad (3)$$

where:

$K$  is a rigid matrix,

$M$  is a mass matrix,

$\omega$  is an eigen-value (frequency), and

$\phi$  is an eigen-vector

With respect to the coordinate system of the  $2 \times 12$ -cell diaphragm, approximations were generated using the physical properties and coordinate system shown in Table 1 for three components--the copper coils, the base resin of the film and the edges. For the Young's modulus of the base resin, which was not available from the literature, we used measured values obtained from tension tests.

##### 3.2.2 Vibrational Mode Analysis

The eigen-vectors obtained by solving Equation (3) represent displacement vectors and in physical terms signify the vibrational modes of the  $2 \times 12$ -cell diaphragm. Figure

4 shows the results of vibrational mode analysis from the eigen-vectors. In vibration mode 1, the center of the diaphragm is the loop of vibration where the amplitude is the greatest. In vibration mode 2, the center of the diaphragm is the node of vibration where the amplitude is zero. In vibration mode 3, the diaphragm is divided length-wise into three sections and there is a vibration node in two places and a vibration loop in three places. As the number of vibration modes increases the diaphragm is divided into smaller sections and the degrees of freedom of vibration increase.

### 3.2.3 Examination of the Reproduction Band by Eigen-value Analysis

In eigen-value analysis simulations were carried out using the physical properties of the materials of which the diaphragm is composed and the configuration of the components as variables. Eigen-frequencies were derived from the eigen-values calculated by Equation (3) for a variety of prerequisite conditions. The proper-vibration having the lowest frequency is equivalent to the primary vibration mode, and corresponds to  $f_0$ , which has a close relationship to the reproduction band in the bass region.

Figure 5 shows the relationship between the Young's modulus of the edge by which the diaphragm is mounted to the acoustic transducer and the eigen-frequency. It was found that the eigen-frequency increased with a rise in the Young's modulus of the edge in all vibration modes, agreeing with the prediction, based on Equation (2), that

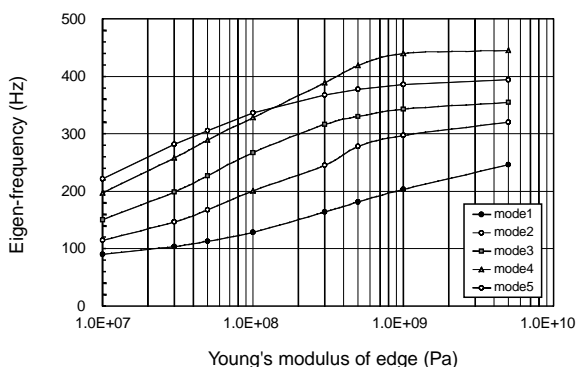


Figure 5 Effect of Young's modulus of edge on eigen-frequency.

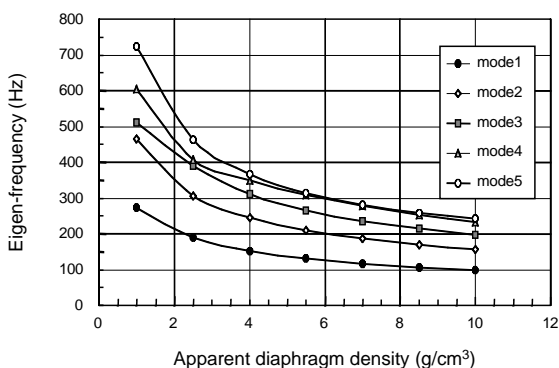


Figure 6 Effect of apparent diaphragm density on eigen-frequency.

as the stiffness of the diaphragm support structure  $s$  increased  $f_0$  would rise. This suggested that the best way of widening the reproduction band in the bass range would be to change to a material with a smaller Young's modulus--that is to say a more flexible material such as rubber or foam--for the edge.

As a means of investigating the relationship between the mass of the diaphragm and its eigen-frequency, we may examine the relationship shown in Figure 6 between apparent diaphragm density (average of values for coils and film) and the eigen-frequency. In Figure 6 the change in the weight of the diaphragm, made up of copper coils and base resin film, was approximated to a change in density and analyzed. It was found that as the weight of the diaphragm increased the eigen-frequency tended to shift to a lower frequency, a result that could be anticipated from Equation (2). This agrees with the predicted result that as equivalent mass of a vibrational system increases  $f_0$  will decrease. This in turn suggests that to broaden the reproduction band in the bass range (i.e., to decrease  $f_0$ ), the design should be modified to increase diaphragm weight by, for example, increasing the amount of copper or using thicker base resin for the film.

We then examined the relationship between the outer configuration of the diaphragm and the eigen-frequency. Figure 7 shows the relationship with eigen-frequency when the length dimension differs in proportion to the number of magnets disposed ( $2 \times n$ ), using identical edge material and diaphragm material. As the number of magnets disposed in the length dimension increased from 2 to 4, 8, 12 and 20, it was found that the eigen-frequency showed a tendency to shift downward. This result means that the greater the length the wider the reproduction band in the bass range, and is in agreement with the accepted rule of thumb for acoustic transducer design.

The simulation techniques that have thus been established for predicting the reproduction frequency band (an important characteristic of acoustic transducer diaphragms) make it possible to reduce the number of prototypes built, and promises to shorten the time that will be required to develop  $2 \times 2$ -,  $3 \times 4$ -,  $4 \times 4$ - and  $4 \times 12$ -cell diaphragms.

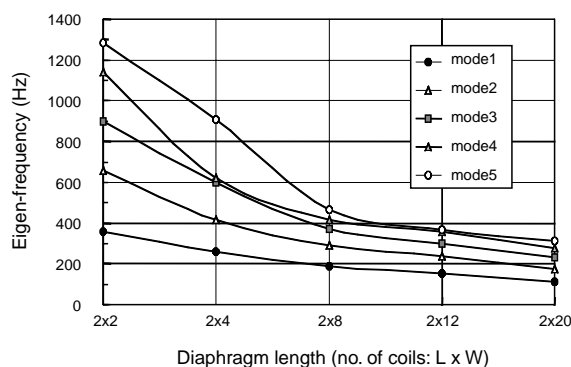


Figure 7 Effect of diaphragm length on eigen-frequency.

## 4. RESULTS AND DISCUSSION

### 4.1 Frequency Characteristics

Prototypes of the 2 x 12-cell diaphragm here under development were fabricated by the subtractive method using a laminated sheet that was copper-clad on both sides, with a base material of heat-resistant plastic film. The acoustic characteristics--sound pressure, impedance, etc.--vs. frequency were measured using an ASA-2 system manufactured by Etani Electric Co., Ltd., with the acoustic transducer attached to a standard baffle as specified in JIS C 5532.

Figure 8 shows the sound pressure level as a function of frequency for diaphragms having a base film 50  $\mu\text{m}$  thick and three types of edge material. The sound pressure characteristics of the prototypes were substantially flat over a wide range of frequencies (200 Hz to 20 kHz), irrespective of the edge material used. However, as indicated by the arrow, in the bass range below 200 Hz there were marked differences depending on the edge material.

Figure 9 is analogous to Figure 8, showing the results of impedance measured for the diaphragms. For planar acoustic transducers using a urethane edge, the  $f_0$  was 163 Hz, while the values for planar acoustic transducers using edges of compressed foam rubber 5 mm and 4 mm thick were 135 Hz and 113 Hz respectively. Other than the

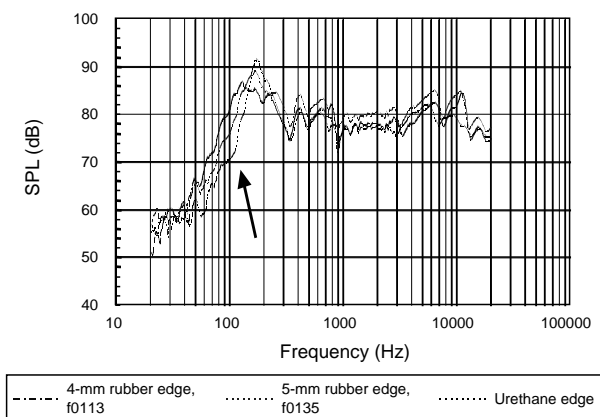


Figure 8 Sound pressure level as a function of frequency. (0.5 W, 50 cm)

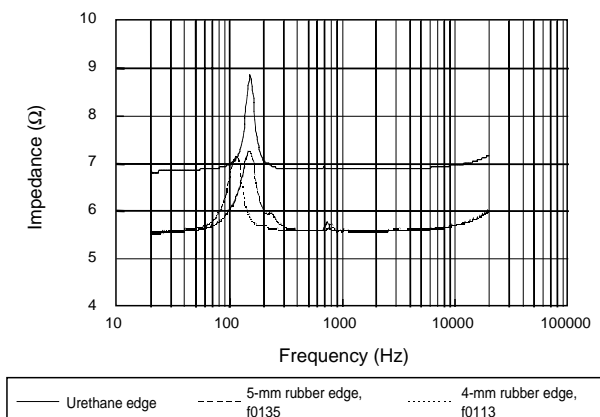


Figure 9 Impedance as a function of frequency. (0.5 W, 50 cm)

edges, these three types of diaphragms were identical in terms of base film and copper coils, so that it may be concluded that the differences in  $f_0$  are attributable to the physical properties of the edge materials. Thus it was confirmed that, as was predicted by the simulation shown in Figure 5, the reproduction band in the bass range can be designed by controlling the stiffness of the edge material.

In an effort to improve the sound characteristics, the investigation was pursued by fabricating prototype diaphragms of varying materials and configurations, as described above, and in parallel, by recreating these characteristics by simulation. This resulted in improvements in the circuit configuration and edge materials of the 2 x 12-cell diaphragm (the details of which are omitted here) such that a sound pressure of 65 dB or better was achieved. Further, through the development of band design techniques whereby trends in  $f_0$  and reproduction band can be predicted by eigen-frequency simulation, it has become possible to predict the characteristics of diaphragms of differing configurations.

### 4.2 Vibration Characteristics

#### 4.2.1 Vibration Measurement System

In the diaphragm developed here, the voice coils formed on the printed circuit vibrate integrally as the diaphragm, with the result that it was necessary to establish the reliability of the diaphragm against open circuit faults--a problem that did not arise with conventional cone speakers. A PSV-100 laser scanning Doppler vibrometer system made by Polytech of Germany was therefore used to gain an understanding of the vibrational characteristics of the diaphragm. Figure 10 shows a schematic representation of the system.

The frequency response function was measured by directing a laser beam against the center of the vibrating diaphragm of a planar acoustic transducer, converting the speed information obtained from the Doppler effect of the reflected laser light, and performing frequency analysis. In laser scanning vibrometry the beam was directed to an array of 8 x 32 points distributed over the entire surface of the diaphragm and time synchronized to yield phase information, and frequency analysis was carried out.

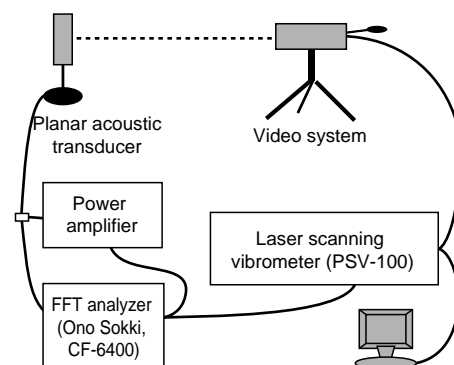


Figure 10 Schematic diagram of vibration measurement system.

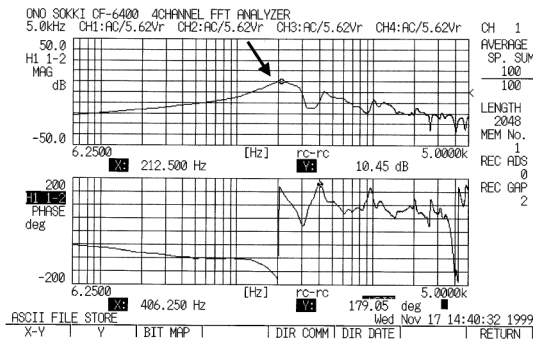


Figure 11 Frequency response function.

#### 4.2.2 Frequency Response Function

Figure 11 shows typical measurements of the frequency response function in a 2 x 12-cell diaphragm. The maximum or peak value of the function was measured in the vicinity of  $f_0$ , and it was found that the peak frequency depended on terminal voltage. This is attributed to the occurrence, in a diaphragm gently constrained by the edge, of non-linear phenomena such as distortion and split vibration that were dependent on terminal voltage.

#### 4.2.3 Vibrational Mode Measurement

Figure 12 shows measurement of the vibration mode at a phase angle of 90°C when inputting a frequency in the vicinity of  $f_0$ . In the vibration mode shown in Figure 12, phase is coincident over the entire surface of the diaphragm, and it will be seen that this corresponds to Mode 1 in the simulation in Figure 4.

When the frequency of laser light reflected from the diaphragm was analyzed, a frequency distribution equivalent to the second and third harmonics of the input frequency was measured, signifying that when frequency  $f_0$  was input vibration in Mode 2 and Mode 3 resulting from distortion etc. were co-present with Mode 1.

Figure 13 also shows a case in which more than one vibration mode is thought to be present, where the primary component of vibration is thought to be Mode 3<sup>4)</sup>.

#### 4.2.4 Features of the Planar Acoustic Transducer Diaphragm

The vibration behavior of the planar acoustic transducer diaphragm was measured directly by laser Doppler vibrometry, and it was concluded that reciprocating motion occurred over the entire flat surface of the diaphragm, as exemplified in Figure 12. This is attributed to the fact that since the voice coils were formed over the entire diaphragm surface, the planar acoustic transducer acts as an area sound source. Thus it is to be expected that the planar acoustic transducer will be characterized by flat phase and sharp directionality. When actual acoustic transducer performance was checked it was discovered that, in addition to the predicted advantages, howling did not occur readily due to the small size of the cells, and that underwater operation was possible thanks to the high level of water resistance.

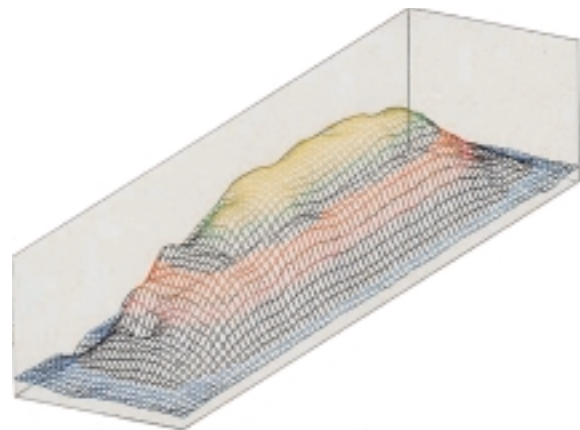


Figure 12 Measurement of vibration. (Case I)

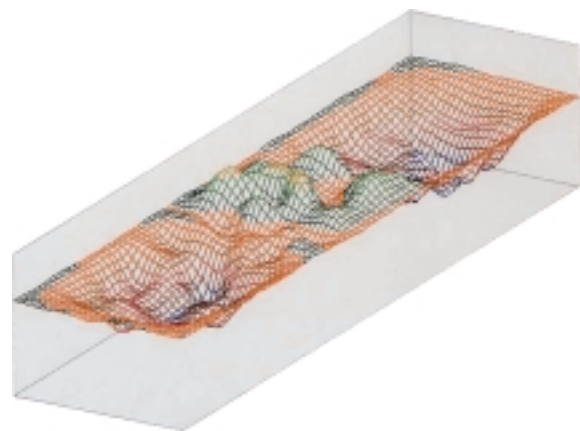


Figure 13 Measurement of vibration. (Case II)

### 4.3 Results of Reliability Tests

The reliability tests listed in Section 2.1 as required for ordinary acoustic transducers were carried out, and it was confirmed that no problems occurred under any conditions.

## 5. CONCLUSION

A 2 x 12-cell diaphragm was developed for use in a planar acoustic transducer having a thickness of 1 cm or less.

(1) Sophisticated circuit design techniques for the sound characteristics were established through the use of magnetostatic analysis, determining areas of high magnetic field density from the arrangement of magnets on the yoke and allocating the two-dimensional wiring space on the diaphragm.

(2) By modeling the diaphragm, simulation of eigen-frequencies was carried out and it was confirmed that there was a correlation between the measured frequency characteristics and the eigen-frequencies. In this way band design techniques were developed for predicting the reproduction band in the bass range from the physical properties of materials and the outline dimensions.

(3) Vibrational mode analysis was carried out by laser Doppler vibrometry, confirming the full-surface driving capability (area sound source) that is characteristic of planar acoustic transducers, and phase flatness.

It has thus been possible to develop and bring to commercial viability a diaphragm that provides a satisfactory reproduction band in the bass range and satisfies all reliability tests established for planar acoustic transducers.

In closing the authors would like to express their heartfelt thanks to Toshiiku Miyazaki and Masashi Hori of FPS Co., Ltd. for their cooperation in designing circuitry and providing components.

#### REFERENCES

- 1) Tamon Saeki: Encyclopedia of speakers and enclosures, Seibundo-Shinkosha, (1999), 52. (in Japanese)
- 2) International patent disclosure, WO99/03304
- 3) Shoji Hori; What is a multi-cell flat speaker?, JAS journal, No. 3, Vol. 40, (2000), 13-16. (in Japanese)
- 4) Nobuo Tanaka: Plate vibration and sound radiation, Noise Control, No. 5, Vol. 11 (1998), 243-247. (in Japanese)

Manuscript received on July 2, 2001.